

1 **Effect of mid-term drought on *Quercus pubescens* BVOCs** 2 **emissions seasonality and their dependence to light and/or** 3 **temperature**

4 Amélie Saunier¹, Elena Ormeño¹, Christophe Boissard², Henri Wortham³, Brice Temime-
5 Roussel³, Caroline Lecareux¹, Alexandre Armengaud⁴, Catherine Fernandez¹.

6 ¹Aix Marseille Univ, Univ Avignon, CNRS, IRD, IMBE, Marseille, France.

7 ²Laboratoire des Sciences du Climat et de l'Environnement, LSCE/IPSL, CEA-CNRS-UVSQ, Université Paris-
8 Saclay, F-91191 Gif-sur-Yvette, France.

9 ³Aix Marseille Univ, CNRS, LCE, Laboratoire de Chimie de l'Environnement, Marseille, France

10 ⁴ Air PACA, 146 rue Paradis, Bâtiment Le Noilly Paradis, 13294 Marseille, Cedex 06.

11 *Correspondence to:* Amélie Saunier (amelie.saunier@imbe.fr)

12 **Key words:** BVOCs, natural and amplified drought, season, light and temperature

13 **Abstract.** Biogenic volatile organic compounds (BVOCs) emitted by plants represent a large source of carbon
14 compounds released into the atmosphere where they account for precursors of tropospheric ozone and secondary
15 organic aerosols. Being directly involved in air pollution and indirectly in climate change, understanding what
16 factors drive BVOC emissions is a prerequisite for modelling their emissions and predict air pollution. The main
17 algorithms currently used to model BVOCs emissions are mainly light and/or temperature dependent. Additional
18 factors such as seasonality and drought also influence isoprene emissions, especially in the Mediterranean region
19 which is characterized by a rather long drought period in summer. These factors are increasingly included in
20 models but only for the principal studied BVOC, namely isoprene but there are still some discrepancies in
21 estimations of emissions. In this study, the main BVOCs emitted by *Quercus pubescens*: isoprene, methanol,
22 acetone, acetaldehyde, formaldehyde, MACR, MVK and ISOPOOH (these 3 last compounds detected under the
23 same ion), were monitored with a PTR-ToF-MS over an entire seasonal cycle, under both *in situ* natural and
24 amplified drought which is expected with climate change. Amplified drought impacted all studied BVOCs by
25 reducing emissions in spring and summer while increasing emissions in autumn. All six BVOCs monitored
26 showed daytime light and temperature dependencies while three BVOCs (methanol, acetone and formaldehyde)
27 also showed emissions during the night despite the absence of light under constant temperature. Moreover,
28 methanol and acetaldehyde burst in the early morning and formaldehyde deposition/uptake were also punctually
29 observed which were not assessed by the classical temperature and light models.

30 **1 Introduction**

31 Plants contribute to global emissions of volatile organic compounds (VOCs) with an estimated emission rate of
32 10^{15} gC yr⁻¹ (Guenther *et al.* 1995; Harrison *et al.* 2013). The large variety of compounds released by plants
33 represents, at the global scale, 2-3% of the total carbon released in the atmosphere (Kesselmeier & Staudt 1999).
34 Under strong photochemical conditions, BVOCs, together with NO_x, can significantly contribute to tropospheric
35 ozone concentration (Xie *et al.* 2008; Papiez *et al.* 2009). In addition to its greenhouse effect, O₃ has strong
36 effects on plant metabolism (Reig-Armiñana *et al.* 2004; Beauchamp *et al.* 2005) as well as on human health
37 (Lippmann 1989). BVOCs are also rapidly oxidized by OH radical and NO₃ (Hallquist *et al.* 2009; Liu *et al.*
38 2012), which account for an important fraction of the total mass of secondary organic aerosols (SOA, Jimenez *et al.*
39 *et al.* 2009). Methanol and acetone are, after isoprene, the principal BVOC released to the atmosphere. Isoprene
40 emissions represent between 400-600 TgC yr⁻¹ at the global scale (Arneeth *et al.* 2008) whereas methanol
41 emissions vary between 75 and 280 TgC yr⁻¹ (Singh *et al.* 2000; Heikes *et al.* 2002, respectively) and acetone
42 emissions represent only 33 TgC yr⁻¹ (Jacob *et al.* 2002). Other compounds such as acetaldehyde, methacrolein
43 (MACR), methyl vinyl ketone (MVK), isoprene hydroxy hydroperoxides (ISOPOOH) and formaldehyde, whose
44 biogenic origin has been poorly investigated, are better known to be anthropogenic and/or secondary VOCs
45 issued from atmospheric oxidations (Hallquist *et al.* 2009). However, acetaldehyde is also a by-product of plant
46 metabolism and its emissions represent 23 Tg yr⁻¹ at the global scale (Millet *et al.* 2010). Formaldehyde, MACR,
47 MVK and ISOPOOH are released by plants through oxidations of methanol and isoprene, respectively, within
48 leaves but they can have other leaf precursors (Oikawa & Lerdau 2013). Thus, it is thereby important to model
49 all this panel of BVOCs emissions with the aim of predicting their effect on secondary atmospheric chemistry.
50 Current models allow to predict BVOCs emissions according to the type of vegetation, biomass density, leaf age,
51 specific emission factor for many vegetal species, as well as the impact of some environmental factors. Models,
52 such as the MEGAN (Guenther *et al.* 2006; Guenther *et al.* 2012) or CHIMERE (Menuet *et al.* 2014) model,
53 include at least two main algorithms that allow to model light and temperature emissions dependence (called
54 *L+T* algorithm afterwards) and a temperature dependent algorithm (called *T* algorithm afterwards), both
55 described in Guenther *et al.* (1995). The *L+T* algorithm is typically used for BVOCs emissions whose synthesis
56 rapidly relies on photosynthesis, and hence include *de novo* emissions. The *T* algorithm is used for BVOCs
57 emissions that do not directly rely on BVOCs synthesis when, for example, they originate from permanent large
58 storage pools (Ormeno *et al.* 2011). The dependence to light and/or temperature is well documented for
59 isoprenoids (Owen *et al.* 2002; Rinne *et al.* 2002; Dindorf *et al.* 2006) but there is still a lack of knowledge about
60 highly volatile BVOCs (e.g. methanol, acetone, acetaldehyde). However, many of these compounds are very
61 reactive in the atmosphere (Hallquist *et al.* 2009) and, could be emitted in large quantities to the atmosphere at
62 global scale. The characterization of their emissions and sensitivity to light and/or temperature is, thus, necessary
63 in order to obtain reliable predictions of atmospheric processes in order not to miss this important part of the
64 atmospheric reactivity.

65 Other factors than light and temperature can drive BVOCs emissions such as water stress. Most studies dealing
66 with BVOCs response to water stress have, however, focused on terpene-like compounds and have been carried
67 out after weeks of watering restriction or removal under controlled conditions (for a review, see studies cited in
68 Peñuelas and Staudt 2010). Considerable uncertainty remains in our understanding of emission mechanisms
69 since some works showed increases (Funk *et al.* 2004; Monson *et al.* 2007) or decreases of isoprene emissions
70 (Brüggenmann & Schnitzler 2002; Fortunati *et al.* 2008) and there is a lack of knowledge on the impact of water

71 stress on highly BVOCs emissions. Moreover, the understanding of sensitivity of isoprene and highly volatile
72 BVOCs emissions to recurrent water stress (few years) under *in situ* conditions is clearly missing. Likewise, the
73 capacity of current *L+T* and *T* algorithms to predict emission shifts under different drought scenarios in the
74 context of climate change needs to be addressed for isoprene and highly volatile compounds. This is of especial
75 interest for the Mediterranean area where the most severe climatic scenario of the IPCC predicts an
76 intensification of summer drought consisting on a rain reduction that can locally reach 30%, an extension of the
77 drought period as well as a temperature rise of 3.4°C, (Giorgi & Lionello 2008; IPCC 2013; Polade *et al.* 2014)
78 for 2100.

79 In the present investigation, we aimed (i) to study the standard emission factors of each studied BVOC released
80 by *Q. pubescens*, including isoprene and highly volatile compounds that originate from plant metabolism under
81 water stress (ii) to test the performance of the *L+T* and *T* algorithms to predict isoprene and highly volatile
82 BVOCs emissions over the seasonal cycle and under two recurrent water stress treatments. *Q. pubescens* was
83 chosen as vegetal model because this species is highly resistant to drought and well widespread in the Northern
84 Mediterranean area occupying 2 million ha (Quézel & Médail 2003). It also represents the major source of
85 isoprene emissions in the Mediterranean area and the second one at the European scale (Keenan *et al.* 2009).

86 **2 Material and methods**

87 **2.1 Experimental site**

88 Our study was performed at the O₃HP site (Oak Observatory at OHP, Observatoire de Haute Provence), located
89 60 km North of Marseille, France (5°42'44" E, 43°55'54" N), at an elevation of 650m above the sea level. The
90 O₃HP (955m²), free from direct human disturbance for 70 years, consists of a homogeneous forest mainly
91 composed of *Q. pubescens* (≈ 90 % of the biomass and ≈ 75 % of the trees) with a mean diameter of 1.3 m. The
92 remaining 10 % of the biomass is mainly represented by *Acer monspessulanum* trees, a very low isoprene-
93 emitter species (Genard-Zielinski *et al.* 2015). The O₃HP site was created in 2009 in order to study the impact of
94 climate change on a *Q. pubescens* forest. Using a rainfall exclusion device (an automated monitored roof
95 deployed during rain events) set up over part of the O₃HP canopy, it was possible to reduce natural rain by 30%
96 and to extend the drought period in an attempt to mimic the current climatic model projections for 2100 (Giorgi
97 & Lionello 2008; IPCC 2013; Polade *et al.* 2014). Two plots were considered in the site; a plot receiving natural
98 precipitation where trees grew under natural drought (300m² surface, used as control plot) and a second plot
99 submitted to amplified drought (232m² surface). Rain exclusion on this latter plot started on April 2012 and was
100 continuously applied every year, principally, during the growth period. Ombrothermic diagrams indicated that
101 the drought period was extended for 2 months in 2012, 4 months in 2013 and 3 months in 2014 for amplified
102 drought relative to natural drought (Fig 1). Data on cumulative precipitation showed that 35% of rain was
103 excluded in 2012 (from 29 April from to 27 October), 33.5% in 2013 (from 7 July from to 29 December), 35.5%
104 in 2014 (from 8 April to 8 December). This experimental set up involved a recurrent drought in the amplified
105 drought plot. Sampling was performed at the branch-scale at the top of the canopy during three campaigns from
106 October 2013 to July 2014, covering an entire seasonal cycle: in autumn (14 to 28 October 2013, 2nd year of
107 amplified drought), in spring (12 to 19 May 2014, 3rd year of amplified drought) and in summer (13 to 25 July
108 2014, 3rd year of amplified drought). Spring, summer and autumn campaigns corresponded to the end of leaf

109 growth, leaf maturation and the beginning of the leaf senescence, respectively. The same five trees per plot were
110 selected and investigated throughout the study.

111 **2.2 Branch scale-sampling methods**

112 Two identical dynamic branch enclosures were used for sampling gas exchange (in terms of CO₂, H₂O and
113 BVOCs) as fully described in Genard-Zielinski *et al.* (2015) with some modifications. Branches were enclosed
114 in a \approx 30L PTFE (polytetrafluoroethylene) frame closed by a 50 μ m thick PTFE film. One tree from natural and
115 one tree from amplified drought plot were analysed concomitantly during 1 or 2 days. Inlet air was introduced at
116 9L.min⁻¹, controlled by mass flow controllers (MFC, Bronkhorst), using a pump, inside, by PTFE (KNF
117 N840.1.2FT.18®, Germany) allowing for air renewal inside the chamber every \sim 3min. Ozone was removed
118 from inlet air by placing PTFE filters impregnated with sodium thiosulfate (Na₂S₂O₃) as described by Pollmann
119 *et al.* (2005), so that oxidation of BVOCs due to ozone within the enclosed atmosphere is negligible. The excess
120 of air humidity was removed using drierite. A PTFE fan ensured a rapid mixing of the chamber air and a slight
121 positive pressure within the enclosure enabled the PTFE film to be held away from leaves to minimise biomass
122 damage. Microclimate (temperature, relative humidity and photosynthetically active radiation or PAR) was
123 continuously (every minute) monitored by a data logger (LI-COR 1400®; Lincoln, NE, USA) with a relative
124 humidity and temperature probe placed inside the chamber (RHT probe, HMP60, Vaisala, Finland) and a
125 quantum sensor (PAR, LI-COR, PAR-SA 190®, Lincoln, NE, USA) placed outside the chamber. The climatic
126 conditions in terms of PAR and temperatures are summarized in Fig. S1 (in supplementary files) for each field
127 campaigns. All air flow rates were controlled by mass flow controllers (MFC, Bronkhorst) and all tubing lines
128 were made of PTFE. Chambers were installed the day before measurements and flushed overnight. Enclosed
129 branches contained 8 to 12 leaves corresponding to a range of 1.4 to 3.6g of dry matter and 110 to 320cm² of leaf
130 surface, respectively

131 **2.3 Ecophysiological parameters**

132 Exchange of CO₂ and H₂O from the enclosed branches was continuously (every min) measured using infrared
133 gas analysers (IRGA 840A®, LI-COR) concomitantly with BVOCs emission measurements (cf. 2.4). Gas
134 exchange values were averaged by taking into account all the data measured between 12h and 15h (local time).
135 Net photosynthesis (P_n , μ molCO₂ m⁻² s⁻¹) and stomatal conductance to water (G_w , mmolH₂O m⁻² s⁻¹) were
136 calculated using equations described by Von Caemmerer and Farquhar (1981) as used in Genard-Zielinski *et al.*
137 (2015) (for more details, see Appendix A, equations A1 to A4). Leaves from enclosed branches were directly
138 collected after gas exchange sampling to accurately measure leaf surface with a leaf area meter. P_n and G_w were
139 hence expressed in a leaf surface basis. After that, leaves were freeze-dried to assess their dry mass.

140 **2.4 BVOCs analysis**

141 A PTR-ToF-MS 8000 instrument (Ionicon Analytik GmbH, Innsbruck, Austria) was used for online
142 measurements of BVOCs emitted by the enclosed branches. A multi-position common outlet flow path selector
143 valve system (Vici) and a vacuum pump were used to sequentially select air samples from: amplified drought,
144 inlet air, natural drought, ambient air and catalyst. The catalyst consists in a 25 cm long stainless steel tubing,

145 filled with platinum wool and heated at 350°C to efficiently remove VOCs from sample and measure potential
 146 instrumental background levels. Each sample was analysed every hour, with 15min of analysis. Mass spectra in
 147 the range 0-500amu were recorded at 1min integration time. The reaction chamber pressure was fixed at
 148 2.1mbar, the drift tube voltage at 550V and the drift tube temperature at 313 K corresponding to an electric field
 149 strength applied to the drift tube (E) to a buffer gas density (N) ratio of 125Td (1Td = 10⁻¹⁷ V cm²). A calibration
 150 gas standard, consisting of a mixture of 14 aromatic organic compounds (TO-14A Aromatic Mix, Restek
 151 Corporation, Bellefonte, USA, 100 ± 10ppb in Nitrogen), was used to experimentally determine the ion relative
 152 transmission efficiency. BVOCs targeted in this study and their corresponding ions include formaldehyde (m/z
 153 31.018), methanol (m/z 33.033), acetaldehyde (m/z 45.03), acetone (m/z 59.05), isoprene (m/z 41.038, 69.069)
 154 and MACR+MVK+ISOPOOH (m/z 71.049, these three compounds were detected with the same ion with PTR-
 155 MS). The signal corresponding to protonated VOCs was converted into mixing ratios by using the proton
 156 transfer rate constants k given by Cappellin *et al.* (2012). Formaldehyde concentrations were calculated
 157 according to the method described by Vlasenko *et al.* (2010) to account for its humidity dependent sensitivity.
 158 BVOCs emissions rates (ER) were calculated by considering the BVOCs concentrations in the inlet and outlet
 159 air as follows (equation 1):

$$160 \quad ER = \frac{Q_0 * (C_{out} - C_{in})}{B} \quad (1)$$

161 where ER was expressed in µgC g_{DM}⁻¹ h⁻¹, Q₀ was the flow rate of the air introduced into the chamber (L h⁻¹),
 162 C_{out} and C_{in} were the concentrations in the inflowing and outflowing air (µgC L⁻¹), respectively, and B was the
 163 total dry biomass matter (g_{DM}). Daily cycles were made by averaging measured emissions of all trees every hour.

164 2.5 Emission algorithms

165 The light and/or temperature dependence of *Q. pubescens* BVOCs (isoprene and highly volatile compounds)
 166 under natural and amplified drought was tested using both the L+T and T algorithms. Emission rates calculated
 167 according to these algorithms (called afterwards ER_{L+T} and ER_T, respectively) were calculated using the equation
 168 described in Guenther *et al.* (1995) (for more details, see Appendix B, equations B1 to B5). The empirical
 169 coefficient β (used in the T algorithm) was determined for each compound according to the season and the
 170 treatment through the slope of correlation between the natural logarithm of emissions rates (measured emissions,
 171 µgC g_{DM}⁻¹ h⁻¹) and experimental temperature (K). Standardised emissions rates (EF, emissions rates at standard
 172 conditions of light and temperature, 1000µmol m⁻² s⁻¹ and 30°C), were used to calculate modelled emissions. EF
 173 were determined for each compound according to the season and the treatment and corresponded to the slope of
 174 the correlation between experimental emission rates and values of C_i*C_i when using the L+T algorithm or C_T
 175 when using the T algorithm (see Appendix B for a full description of C_i*C_i and C_T). All parameters used for the
 176 calculation of modelled emissions are presented in supplementary files (Table S1).

177 2.6 Data treatment

178 Data treatment was performed with the software STATGRAPHICS® centurion XV (Statpoint, Inc). After
 179 having checked the normality of the data set, two-way repeated measures ANOVA were performed to evaluate
 180 the variability of Pn, Gw and BVOC emission rates according to the drought treatment and the season. Pearson's
 181 correlations between measured and modelled emissions were performed to evaluate the algorithm (L+T or T)

182 that better predicted *Q. pubescens* emissions under the different drought conditions and over the seasonal cycle.
183 Afterwards, linear regressions tests and slope comparison tests (equal to 1, referred to “sl” afterwards) were also
184 performed to evaluate the good fit of tested algorithms with BVOC emissions rates.

185 **3. Results and discussion**

186 **3.1 Ecophysiological parameters**

187 The physiology of *Q. pubescens* was slightly impacted by amplified drought (Fig. 2), over the whole study, with
188 a decrease of G_w under amplified drought compared to natural drought, by 44 % in spring ($P < 0.1$) and 55 % in
189 summer ($P < 0.01$, Table 1). In autumn, there was no significant difference between both treatments. P_n was
190 only reduced in summer by 36 % ($P < 0.1$) and there was no difference for the others season. Thus, the stomatal
191 closure observed had a slight impact on carbon assimilation. Indeed, *Q. pubescens* has a high stem hydraulic
192 efficiency (Nardini & Pitt 1999) which compensates the stomatal closure since it allows to use water more
193 efficiently, thus, maintaining P_n . Moreover, it must be noted that an increase of P_n was observed in autumn and
194 could likely be attributed to the autumnal rains. These results showed that the amplified drought artificially
195 applied to *Q. pubescens* at O₃HP led to a moderate drought for this species, based on a moderate reduction of the
196 physiological performances (Niinemets 2010).

197 **3.2 Effect of drought on BVOCs emissions**

198 The emissions of all BVOCs followed during this experimentation were reduced under amplified drought
199 compared to natural drought, especially in spring and summer (Table 1) except for acetaldehyde emissions.
200 Indeed, for this compound, there was no significant difference between both treatments probably due to a large
201 variability of the data set. In autumn, for all BVOCs, there was no difference between both plots. The decrease of
202 oxygenated BVOCs in spring and summer under amplified drought (e.g. methanol, MACR+MVK+ISOPOOH,
203 formaldehyde, acetone) could be explained by the stomatal closure in spring and summer under amplified
204 drought. Indeed, the emissions of these compounds are strongly bound to G_w (Niinemets *et al.* 2004). Isoprene
205 emissions were also reduced in spring and summer during the third year of this experiment whereas an increase
206 was observed in the first year (personal communication from A.C Génard-Zielinski) as well as what had been
207 shown by Brüggemann and Schnitzler (2002) but this work was conducted with potted plants. The isoprene
208 decrease observed in our experiment cannot be explained by the stomatal closure because this compound could
209 also be emitted through the cuticle (Sharkey & Yeh 2001). It could rather be due to the decrease of P_n which
210 reduced the carbon availability to produce isoprene. Moreover, carbon assimilated through P_n can be also
211 invested into the synthesis of other defense compounds leading to a decrease of isoprene production and
212 emission.

213 **3.3 Effect of drought on light and/or temperature dependence through a seasonal cycle**

214 All six BVOCs monitored showed daytime light and temperature dependencies (isoprene, degradation products
215 of isoprene and acetaldehyde), while three BVOCs (methanol, acetone and formaldehyde) also showed
216 emissions during the night despite the absence of light under constant temperature.

217

218 Regarding the light and temperature dependencies, the daily cycle of isoprene emissions (Fig. 3) showed that this
219 compound responds strongly to light and temperature as already known (Guenther *et al.* 1993) and that this
220 response was not impacted by amplified drought. Isoprene can protect thylakoids from oxidative damage
221 (Velikova *et al.* 2011) occurring mainly during the day which can explain this kind of dependence. Yet, our
222 results showed the importance to take into account the effect of amplified drought on emission factors because
223 the intensity of isoprene emissions between natural and amplified drought was very different independently of
224 the season. The modelled emissions were very representative of measured emissions except in spring for natural
225 drought when we obtained a slight underestimation of emissions ($sl = 0.84$, $P < 0.05$) maybe, because light and
226 temperature, in spring, were not the only parameters driving isoprene emissions. At this season, plants likely
227 needed to produce more isoprene to protect the establishment of photosystems in the new leaves.

228 MACR+MVK+ISOPOOH emissions, as isoprene, seemed to respond better to light and temperature than to only
229 temperature (Fig. S2 in supplementary files) since correlations between measured emissions and ER_{L+T} were
230 always better than correlations with ER_T . Since MACR+MVK+ISOPOOH are oxidation products of isoprene
231 (Oikawa & Lerdau 2013), it is not surprising that these compounds followed the same pattern than isoprene in
232 terms of dependence to light and temperature. The estimations of ER_{L+T} were quite good except in spring under
233 natural drought where a slight underestimation was observed ($sl = 0.87$, $P < 0.05$).

234 The dependence of acetaldehyde emissions to light and/or temperature is very contrasted; studies have shown
235 that they are bound to both light and temperature (Jardine 2008; Fares *et al.* 2011) or to temperature only
236 (Hayward *et al.* 2004). Our results suggested that acetaldehyde emissions were mainly bound to light and
237 temperature (Fig. 4). Indeed, correlations between measured and ER_{L+T} were always better than with ER_T .
238 However, some discrepancies were observed. Under natural drought, underestimations were observed in spring
239 and summer ($sl = 0.72$, and $sl = 0.57$, $P < 0.05$, respectively) whereas in autumn, there was a good estimation (sl
240 $= 0.86$, $P > 0.05$). Under amplified drought, underestimation was only observed in summer ($sl = 0.80$, $P < 0.05$).
241 Daily cycles of acetaldehyde emissions presented also an emissions burst in the morning (at 7h, local time) in
242 spring (under both treatments) and in summer (only under natural drought). Acetaldehyde can be produced due
243 to an overflow of pyruvic acid during light-dark transitions. Cytosolic pyruvic acid levels rise rapidly and it can
244 be converted into acetaldehyde by pyruvate decarboxylase (Fall 2003). This mechanism could explain the
245 morning burst for this compound and the fact that no emissions during the night was observed.

246

247 We observed emissions of methanol, acetone and formaldehyde during the night under no light and constant
248 temperature (around 20°C, see supplementary files S1). Correlations between ER_{L+T} or ER_T and measured
249 methanol emissions were very similar especially in spring and summer (Fig. 5). However, some observed
250 phenomena suggested that methanol emission was sustained by temperature in the absence of light. Indeed, the
251 burst in the early morning (at 7h, local time), similar to acetaldehyde, was observed when stomata opened in
252 spring and summer, independently of the drought treatment although it was clearer under natural than amplified
253 drought. This burst can be explained by a strong release of this compound that has been accumulated in the
254 intercellular air space and leaf liquid pools (due to the relative high polarity of methanol) at night when stomata
255 are closed (Hüve *et al.* 2007). Moreover, for both drought treatments, methanol emissions during the night were
256 observed at any seasons (especially autumn) which could be explained by nocturnal temperatures (roughly

257 constant) that sufficed to maintain the biochemical processes involved in methanol formation. Methanol
258 emissions, which result from the demethylation of pectin during the leaf elongation, has already been described
259 to be temperature dependent alone (Hayward *et al.* 2004; Folkers *et al.* 2008). However, our results suggest that
260 methanol emissions respond strongly to light and temperature during the day. This kind of diurnal emissions
261 cycle has already been described by Smiatek and Steinbrecher (2006). Our results about daily cycles of acetone
262 emissions (Fig. S3 in supplementary files) showed that this compound responded better to light and temperature
263 than only temperature since correlations were better with ER_{L+T} . Under natural drought, the modelled emissions
264 were well representative of measured emissions in summer. By contrast, in spring and in autumn, slight
265 underestimations were observed ($sl = 0.88$, $P < 0.05$ and $sl = 0.69$, $P < 0.05$, respectively). Under amplified
266 drought, good estimations were observed in summer and autumn but in spring, there was an overestimation of
267 modelled emissions ($sl = 1.27$, $P < 0.05$). Previous studies have shown that acetone rather depends on
268 temperature alone (Fares *et al.* 2011) or to light and temperature (Jacob *et al.* 2002), indicating that its
269 dependence to light and/or temperature remains unclear. During the day, acetone emissions were dependent to
270 light and temperature and emissions still occurred during the night, especially in autumn. Alike methanol,
271 nocturnal temperatures could allow to maintain acetone formation (Smiatek & Steinbrecher 2006). Acetone is a
272 by-product of plant metabolism (Jacob *et al.* 2002) and its production can be enzymatic and non-enzymatic (Fall
273 2003) which can explain these observed differences through the day. We can suppose that acetone emissions
274 observed during the day could come from the enzymatic activity and, on the contrary, during the night, they
275 could come from the non-enzymatic production.

276 Formaldehyde emissions followed the same pattern than methanol and acetone emissions (Fig. S4 in
277 supplementary files), especially in autumn. By considering only the daytime (correlation with $L+T$ modelled
278 emissions), there were good estimations in summer and autumn and a slight underestimation was observed in
279 spring ($sl = 0.89$, $P < 0.05$) for natural drought. Under amplified drought, correlations indicated that $L+T$
280 modelled emissions were well representative of measured emissions, but some negative emissions were observed
281 in summer which suggested a deposition or an uptake of this compound by leaves as already highlighted by Seco
282 *et al.* (2008). This phenomenon could have a role in stress tolerance, since formaldehyde can be catabolised
283 (mainly through oxidations) within leaves leading to CO_2 formation (Oikawa & Lerdau 2013). Emissions during
284 the night suggest that formaldehyde came from another source than oxidation within leaves since oxidations
285 occur mainly during the day due to an excess of light in chloroplasts, principal place of reactive oxygen species
286 production (Asada 2006). Thus, formaldehyde emissions observed during the night could result from, for
287 example, the glyoxylate decarboxylation or the dissociation of 5,10-methylene-THF (Oikawa & Lerdau 2013).

288 4 Conclusion

289 After 3 years of amplified drought, all BVOC emissions were reduced in spring and summer compared to natural
290 drought whereas, in autumn, an increase was observed for some compounds. These results are in opposition with
291 the results obtained after only one year of amplified drought (2012), especially for isoprene, where an increase
292 was observed for this compound (Génard-Zielinski *et al.* in review in Biogeosciences). Amplified drought did
293 not seem to shift the dependence to light and/or temperature which remained unchanged between treatments.

294 Moreover, two different dependence behaviours were found: (i) all six BVOCs monitored showed daytime light
 295 and temperature dependencies while (ii) only three BVOCs (methanol, acetone and formaldehyde) also showed
 296 that their emissions were maintained during the night with no light at rather constant nocturnal temperatures.
 297 Moreover, some phenomena, such as methanol and acetaldehyde emissions bursts in early morning or the
 298 formaldehyde deposition/uptake (formaldehyde), were not assessed by either $L+T$ or T algorithm.

299 **Appendix A: calculation of ecophysiological parameters**

300 Net photosynthesis (P_n , $\mu\text{molCO}_2 \text{ m}^{-2} \text{ s}^{-1}$) was calculated using equations described by Von Caemmerer and
 301 Farquhar (1981) as follows:

$$302 \quad P_n = \frac{F*(Cr-Cs)}{S} - CS * E \quad (A1)$$

303 Where F is the inlet air flow (mol s^{-1}), C_s and C_r are the sample and reference CO_2 molar fraction respectively
 304 (ppm), S is the leaf surface (m^2), $C_s * E$ is the fraction of CO_2 diluted in water evapotranspiration and E (molH_2O
 305 $\text{m}^{-2} \text{ s}^{-1}$ then transformed in $\text{mmolH}_2\text{O m}^{-2} \text{ s}^{-1}$, afterward) is the transpiration rate calculated as follow:

$$306 \quad E = \frac{F*(Ws-Wr)}{S*(1-Ws)} \quad (A2)$$

307 where W_s and W_r are the sample and the reference H_2O molar fraction respectively ($\text{molH}_2\text{O mol}^{-1}$).

308 Stomatal conductance to water (G_w , $\text{molH}_2\text{O m}^{-2} \text{ s}^{-1}$ then transformed in $\text{mmolH}_2\text{O m}^{-2} \text{ s}^{-1}$) was calculated using
 309 the following equation:

$$310 \quad G_w = \frac{E*(1-\frac{Wl-Ws}{2})}{Wl-Ws} \quad (A3)$$

311 where W_l is the molar concentration of water vapour within the leaf ($\text{molH}_2\text{O mol}^{-1}$) calculated as follows:

$$312 \quad W_l = \frac{vpsat}{P} \quad (A4)$$

313 where $Vpsat$ is the saturated vapour pressure (kPa) and P was the atmospheric pressure (kPa).

314 **Appendix B: Modelled emissions calculation**

315 The modelled emissions rates according to light and temperature (ER_{L+T}) or the temperature algorithm (ER_T)
 316 were calculated according to algorithms described in Guenther *et al.* (1995) as follows :

$$317 \quad ER_{L+T} = EF_{L+T} * Cl * Ct \quad (B1)$$

318 where EF_{L+T} is the emission factor at $1000 \mu\text{mol m}^{-2} \text{ s}^{-1}$ of photosynthetically active radiation (PAR) and 30°C
 319 of temperature (obtained with the slope of the correlation between experimental emissions and $Cl * Ct$), Cl and
 320 Ct correspond to light and temperature dependence factors respectively and were calculated with the following
 321 formulae:

$$322 \quad Cl = \frac{\alpha C_{L1} L}{\sqrt{1 + \alpha^2 L}} \quad (B2)$$

$$323 \quad Ct = \frac{\exp\left(\frac{C_{T1}(T-T_s)}{RT_s T}\right)}{1 + \exp\left(\frac{C_{T2}(T-T_M)}{RT_s T}\right)} \quad (B3)$$

324 where $\alpha = 0.0027$, $C_{LI} = 1.066$, $C_{T1} = 95000\text{J mol}^{-1}$, $C_{T2} = 230000\text{J mol}^{-1}$, $T_M = 314\text{K}$ are empirically derived
325 constants, L is the photosynthetically active radiation (PAR) flux ($\mu\text{mol m}^{-2} \text{s}^{-1}$), T is the leaf experimental
326 temperature (K) and T_S is the leaf temperature at standard condition (303K).

327 Modelled emissions according to temperature alone that is ER_T , was calculated as follows:

$$328 \quad ER_T = EF_T * C_T \quad (B4)$$

329 where EF_T is the emission factor at 30°C of temperature (obtained with the slope of the correlation between
330 experimental emissions and C_T) and C_T is a temperature dependence factor calculated as follows:

$$331 \quad C_T = \exp[\beta(T - T_S)] \quad (B5)$$

332 where β is an empirical coefficient (with a standard variation value of 0.09K^{-1} used in literature when not
333 measured) determined, in this study, for each compound according to the season and the treatment through the
334 slope of the correlation between the natural logarithm of measured emissions rates (ER , $\mu\text{gC g}_{\text{DM}}^{-1} \text{h}^{-1}$) and
335 experimental temperature (expressed in K), T is the leaf experimental temperature (K) and T_S is the standard
336 temperature (303K).

337 **Author contribution**

338 AS, EO and CF designed the research and the experimental design. AS, BTR, EO and CF conducted the
339 research. AS, CB, BTR, and CL collected and analyzed the data. AS, EO, CB, HW, BTR, AA and CF wrote the
340 manuscript

341 **Competing interests**

342 The authors declare that they have no conflict of interest.

343 **Acknowledgment**

344 This work was supported by the French National Agency for Research (ANR) through the SecPriMe² project
345 (ANR-12-BSV7-0016-01); Europe (FEDER) and ADEME/PACA for PhD funding. We are grateful to FR3098
346 ECCOREV for the O₃HP facilities (<https://o3hp.obs-hp.fr/index.php/fr/>). We are very grateful to J.-P. Orts, I.
347 Reiter. We also thank all members of the DFME team from IMBE and particularly: S. Greff, S. Dupouyet and A.
348 Bousquet-Melou for their help during measurements and analysis. We thank also, the Université Paris Diderot-
349 Paris7 for its support. The authors thank the MASSALYA instrumental platform (Aix Marseille Université,
350 ice.univ-amu.fr) for the analysis and measurements used in this publication.

351 **References**

- 352 Arneth A., Monson R., Schurgers G., Niinemets Ü. & Palmer P. (2008). Why are estimates of global terrestrial
353 isoprene emissions so similar (and why is this not so for monoterpenes)? *Atmospheric Chemistry and*
354 *Physics*, 8, 4605-4620.
- 355 Asada K. (2006). Production and scavenging of reactive oxygen species in chloroplasts and their functions. *Plant*
356 *physiology*, 141, 391-396.
- 357 Beauchamp J., Wisthaler A., Hansel A., Kleist E., Miebach M., NIINEMETS Ü., Schurr U. & WILDT J. (2005).
358 Ozone induced emissions of biogenic VOC from tobacco: relationships between ozone uptake and
359 emission of LOX products. *Plant, Cell & Environment*, 28, 1334-1343.

360 Brüggemann N. & Schnitzler J.P. (2002). Comparison of Isoprene Emission, Intercellular Isoprene
361 Concentration and Photosynthetic Performance in Water-Limited Oak (*Quercus pubescens* Willd. and
362 *Quercus robur* L.) Saplings. *Plant Biology*, 4, 456-463.

363 Cappellin L., Karl T., Probst M., Ismailova O., Winkler P.M., Soukoulis C., Aprea E., Märk T.D., Gasperi F. &
364 Biasioli F. (2012). On quantitative determination of volatile organic compound concentrations using
365 proton transfer reaction time-of-flight mass spectrometry. *Environmental science & technology*, 46,
366 2283-2290.

367 Dindorf T., Kuhn U., Ganzeveld L., Schebeske G., Ciccioli P., Holzke C., Köble R., Seufert G. & Kesselmeier J.
368 (2006). Significant light and temperature dependent monoterpene emissions from European beech
369 (*Fagus sylvatica* L.) and their potential impact on the European volatile organic compound budget.
370 *Journal of Geophysical Research: Atmospheres*, 111.

371 Fall R. (2003). Abundant oxygenates in the atmosphere: a biochemical perspective. *Chemical reviews*, 103,
372 4941-4952.

373 Fares S., Gentner D.R., Park J.-H., Ormeno E., Karlik J. & Goldstein A.H. (2011). Biogenic emissions from
374 Citrus species in California. *Atmospheric Environment*, 45, 4557-4568.

375 Folkers A., Hüve K., Ammann C., Dindorf T., Kesselmeier J., Kleist E., Kuhn U., Uerlings R. & Wildt J. (2008).
376 Methanol emissions from deciduous tree species: dependence on temperature and light intensity. *Plant*
377 *biology*, 10, 65-75.

378 Fortunati A., Barta C., Brilli F., Centritto M., Zimmer I., Schnitzler J.P. & Loreto F. (2008). Isoprene emission is
379 not temperature-dependent during and after severe drought-stress: a physiological and biochemical
380 analysis. *The Plant Journal*, 55, 687-697.

381 Funk J., Mak J. & Lerdau M. (2004). Stress-induced changes in carbon sources for isoprene production in
382 *Populus deltoides*. *Plant, Cell & Environment*, 27, 747-755.

383 Genard-Zielinski A.-C., Boissard C., Fernandez C., Kalogridis C., Lathière J., Gros V., Bonnaire N. & Ormeño
384 E. (2015). Variability of BVOC emissions from a Mediterranean mixed forest in southern France with a
385 focus on *Quercus pubescens*. *Atmospheric Chemistry and Physics Discussions*, 14, 17225-17261.

386 Giorgi F. & Lionello P. (2008). Climate change projections for the Mediterranean region. *Global and Planetary*
387 *Change*, 63, 90-104.

388 Guenther A., Hewitt C.N., Erickson D., Fall R., Geron C., Graedel T., Harley P., Klinger L., Lerdau M., McKay
389 W.A., Pierce T., Scholes B., Steinbrecher R., Tallamraju R., Taylor J. & Zimmerman P. (1995). A
390 global model of natural volatile organic compound emissions. *Journal of Geophysical Research:*
391 *Atmospheres*, 100, 8873-8892.

392 Guenther A., Jiang X., Heald C., Sakulyanontvittaya T., Duhl T., Emmons L. & Wang X. (2012). The Model of
393 Emissions of Gases and Aerosols from Nature version 2.1 (MEGAN2. 1): an extended and updated
394 framework for modeling biogenic emissions.

395 Guenther A., Karl T., Harley P., Wiedinmyer C., Palmer P. & Geron C. (2006). Estimates of global terrestrial
396 isoprene emissions using MEGAN (Model of Emissions of Gases and Aerosols from Nature).
397 *Atmospheric Chemistry and Physics*, 6, 3181-3210.

398 Guenther A.B., Zimmerman P.R., Harley P.C., Monson R.K. & Fall R. (1993). Isoprene and monoterpene
399 emission rate variability: model evaluations and sensitivity analyses. *Journal of Geophysical Research:*
400 *Atmospheres (1984–2012)*, 98, 12609-12617.

401 Hallquist M., Wenger J., Baltensperger U., Rudich Y., Simpson D., Claeys M., Dommen J., Donahue N., George
402 C. & Goldstein A. (2009). The formation, properties and impact of secondary organic aerosol: current
403 and emerging issues. *Atmospheric Chemistry and Physics*, 9, 5155-5236.

404 Harrison S.P., Morfopoulos C., Dani K., Prentice I.C., Arneth A., Atwell B.J., Barkley M.P., Leishman M.R.,
405 Loreto F. & Medlyn B.E. (2013). Volatile isoprenoid emissions from plastid to planet. *New Phytol.*,
406 197, 49-57.

407 Hayward S., Tani A., Owen S.M. & Hewitt C.N. (2004). Online analysis of volatile organic compound emissions
408 from Sitka spruce (*Picea sitchensis*). *Tree Physiology*, 24, 721-728.

409 Heikes B.G., Chang W., Pilson M.E., Swift E., Singh H.B., Guenther A., Jacob D.J., Field B.D., Fall R. &
410 Riemer D. (2002). Atmospheric methanol budget and ocean implication. *Global Biogeochemical*
411 *Cycles*, 16, 80-1-80-13.

412 Hüve K., Christ M., Kleist E., Uerlings R., Niinemets Ü., Walter A. & Wildt J. (2007). Simultaneous growth and
413 emission measurements demonstrate an interactive control of methanol release by leaf expansion and
414 stomata. *Journal of experimental botany*, 58, 1783-1793.

415 IPCC (2013). In: *Contribution of working group I to the fifth assessment report of the intergovernmental panel on*
416 *climate change*. Cambridge University Press Cambridge.

417 Jacob D.J., Field B.D., Jin E.M., Bey I., Li Q., Logan J.A., Yantosca R.M. & Singh H.B. (2002). Atmospheric
418 budget of acetone. *Journal of Geophysical Research: Atmospheres (1984–2012)*, 107, ACH 5-1-ACH
419 5-17.

420 Jardine J. (2008). Plant physiological and environmental controls over the exchange of acetaldehyde between
421 forest canopies and the atmosphere. *Biogeosciences*, 5.

422 Jimenez J., Canagaratna M., Donahue N., Prevot A., Zhang Q., Kroll J.H., DeCarlo P.F., Allan J.D., Coe H. &
423 Ng N. (2009). Evolution of organic aerosols in the atmosphere. *Science*, 326, 1525-1529.

424 Keenan T., Niinemets Ü., Sabate S., Gracia C. & Peñuelas J. (2009). Process based inventory of isoprenoid
425 emissions from European forests: model comparisons, current knowledge and uncertainties.
426 *Atmospheric Chemistry and Physics Discussions*, 9, 6147-6206.

427 Kesselmeier J. & Staudt M. (1999). Biogenic volatile organic compounds (VOC): an overview on emission,
428 physiology and ecology. *Journal of Atmospheric Chemistry*, 33, 23-88.

429 Lippmann M. (1989). Health effects of ozone a critical review. *Japca*, 39, 672-695.

430 Liu Y., Siekmann F., Renard P., El Zein A., Salque G., El Haddad I., Temime-Roussel B., Voisin D., Thissen R.
431 & Monod A. (2012). Oligomer and SOA formation through aqueous phase photooxidation of
432 methacrolein and methyl vinyl ketone. *Atmospheric Environment*, 49, 123-129.

433 Menut L., Bessagnet B., Khvorostyanov D., Beekmann M., Blond N., Colette A., Coll I., Curci G., Foret G. &
434 Hodzic A. (2014). CHIMERE 2013: a model for regional atmospheric composition modelling.
435 *Geoscientific Model Development*, 6, 981-1028.

436 Millet D.B., Guenther A., Siegel D.A., Nelson N.B., Singh H.B., de Gouw J.A., Warneke C., Williams J.,
437 Eerdekens G. & Sinha V. (2010). Global atmospheric budget of acetaldehyde: 3-D model analysis and
438 constraints from in-situ and satellite observations. *Atmospheric Chemistry and Physics*, 10, 3405-3425.

439 Monson R.K., Trahan N., Rosenstiel T.N., Veres P., Moore D., Wilkinson M., Norby R.J., Volder A., Tjoelker
440 M.G. & Briske D.D. (2007). Isoprene emission from terrestrial ecosystems in response to global
441 change: minding the gap between models and observations. *Philosophical Transactions of the Royal
442 Society of London A: Mathematical, Physical and Engineering Sciences*, 365, 1677-1695.

443 Nardini A. & Pitt F. (1999). Drought resistance of *Quercus pubescens* as a function of root hydraulic
444 conductance, xylem embolism and hydraulic architecture. *New Phytol.*, 143, 485-493.

445 Niinemets Ü. (2010). Mild versus severe stress and BVOCs: thresholds, priming and consequences. *Trends in
446 plant science*, 15, 145-153.

447 Niinemets Ü., Loreto F. & Reichstein M. (2004). Physiological and physicochemical controls on foliar volatile
448 organic compound emissions. *Trends in plant science*, 9, 180-186.

449 Oikawa P.Y. & Lerdau M.T. (2013). Catabolism of volatile organic compounds influences plant survival. *Trends
450 in plant science*, 18, 695-703.

451 Ormeno E., Goldstein A. & Niinemets Ü. (2011). Extracting and trapping biogenic volatile organic compounds
452 stored in plant species. *TrAC Trends in Analytical Chemistry*, 30, 978-989.

453 Owen S., Harley P., Guenther A. & Hewitt C. (2002). Light dependency of VOC emissions from selected
454 Mediterranean plant species. *Atmospheric environment*, 36, 3147-3159.

455 Papiez M.R., Potosnak M.J., Goliff W.S., Guenther A.B., Matsunaga S.N. & Stockwell W.R. (2009). The
456 impacts of reactive terpene emissions from plants on air quality in Las Vegas, Nevada. *Atmospheric
457 Environment*, 43, 4109-4123.

458 Polade S.D., Pierce D.W., Cayan D.R., Gershunov A. & Dettinger M.D. (2014). The key role of dry days in
459 changing regional climate and precipitation regimes. *Scientific reports*, 4.

460 Pollmann J., Ortega J. & Helmig D. (2005). Analysis of atmospheric sesquiterpenes: Sampling losses and
461 mitigation of ozone interferences. *Environmental science & technology*, 39, 9620-9629.

462 Quézel P. & Médail F. (2003). *Ecologie et biogéographie des forêts du bassin méditerranéen*. Elsevier Paris.

463 Reig-Armiñana J., Calatayud V., Cerveró J., Garcia-Breijo F., Ibars A. & Sanz M. (2004). Effects of ozone on
464 the foliar histology of the mastic plant (*Pistacia lentiscus* L.). *Environmental Pollution*, 132, 321-331.

465 Rinne H., Guenther A., Greenberg J. & Harley P. (2002). Isoprene and monoterpene fluxes measured above
466 Amazonian rainforest and their dependence on light and temperature. *Atmospheric Environment*, 36,
467 2421-2426.

468 Seco R., Penuelas J. & Filella I. (2008). Formaldehyde emission and uptake by Mediterranean trees *Quercus ilex*
469 and *Pinus halepensis*. *Atmospheric Environment*, 42, 7907-7914.

470 Sharkey T.D. & Yeh S. (2001). Isoprene emission from plants. *Annual review of plant biology*, 52, 407-436.

471 Singh H., Chen Y., Tabazadeh A., Fukui Y., Bey I., Yantosca R., Jacob D., Arnold F., Wohlfrom K. & Atlas E.
472 (2000). Distribution and fate of selected oxygenated organic species in the troposphere and lower
473 stratosphere over the Atlantic. *Journal of Geophysical Research: Atmospheres (1984–2012)*, 105, 3795-
474 3805.

475 Smiatek G. & Steinbrecher R. (2006). Temporal and spatial variation of forest VOC emissions in Germany in the
476 decade 1994–2003. *Atmospheric Environment*, 40, 166-177.

477 Velikova V., Várkonyi Z., Szabó M., Maslenkova L., Nogues I., Kovács L., Peeva V., Busheva M., Garab G. &
478 Sharkey T.D. (2011). Increased thermostability of thylakoid membranes in isoprene-emitting leaves
479 probed with three biophysical techniques. *Plant Physiology*, 157, 905-916.

480 Vlasenko A., Macdonald A., Sjostedt S. & Abbatt J. (2010). Formaldehyde measurements by Proton transfer
481 reaction–Mass Spectrometry (PTR-MS): correction for humidity effects. *Atmospheric Measurement*
482 *Techniques*, 3, 1055-1062.
483 Von Caemmerer S.v. & Farquhar G. (1981). Some relationships between the biochemistry of photosynthesis and
484 the gas exchange of leaves. *Planta*, 153, 376-387.
485 Xie X., Shao M., Liu Y., Lu S., Chang C.-C. & Chen Z.-M. (2008). Estimate of initial isoprene contribution to
486 ozone formation potential in Beijing, China. *Atmospheric Environment*, 42, 6000-6010.

487

488

489

490

491

492

493

494

495

496

497

498

499

500

501

502

503

504

505

506

507

508

509

510

511

512

513 **Table:**

514 **Table 1:** Net photosynthesis (P_n , $\mu\text{molCO}_2 \text{ m}^{-2} \text{ s}^{-1}$), stomatal conductance to water (G_w , $\text{mmolH}_2\text{O m}^{-2} \text{ s}^{-1}$) and emission rates ($\mu\text{gC g}_{\text{DM}}^{-1} \text{ h}^{-1}$) according to treatment and
 515 season. Values represent an average of all data measured between 12h and 15h (local time). Letters denote the difference between drought treatments with $a > b$ and values
 516 showed represent the mean \pm SE, $n=5$. ND: natural drought and AD: amplified drought with ns = non-significant, (*) = $0.05 < P < 0.1$, * = $0.01 < P < 0.05$, ** = $0.001 < P <$
 517 0.01 ,

Season	Spring			Summer			Autumn		
Treatments	ND	AD	<i>P</i>	ND	AD	<i>P</i>	ND	AD	<i>P</i>
Pn	11 \pm 1 a	9 \pm 2 a	ns	14 \pm 2 a	9 \pm 1.2 b	(*)	7 \pm 1 a	9 \pm 1 a	ns
Gw	110 \pm 19 a	57 \pm 13 b	(*)	285 \pm 38 a	126 \pm 17 b	**	122 \pm 23 a	74 \pm 21 a	ns
Isoprene	20 \pm 4 a	10 \pm 2 b	*	124 \pm 10 a	81 \pm 11 b	*	3 \pm 1 a	5 \pm 2 a	ns
MACR+MVK+ISOPOOH	0.1 \pm 0.03a	0.1 \pm 0.01 a	ns	0.4 \pm 0.1 a	0.2 \pm 0.02 b	*	0.04 \pm 0.01 a	0.1 \pm 0.01 a	ns
Methanol	1 \pm 0.1 a	0.5 \pm 0.04 b	*	1 \pm 0.2 a	0.6 \pm 0.03 b	*	0.2 \pm 0.03 a	0.2 \pm 0.1 a	ns
Acetaldehyde	1 \pm 0.4 a	1 \pm 0.3 a	ns	2 \pm 0.5 a	1 \pm 0.1 a	ns	1 \pm 0.3 a	1 \pm 0.3 a	ns
Acetone	0.5 \pm 0.1 a	0.2 \pm 0.02 a	ns	1 \pm 0.2 a	0.5 \pm 0.04 b	**	0.4 \pm 0.1 a	0.4 \pm 0.1 a	ns
Formaldehyde	0.2 \pm 0.05 a	0.1 \pm 0.01 a	ns	0.4 \pm 0.1 a	0.1 \pm 0.02 b	**	0.2 \pm 0.1 a	0.3 \pm 0.1 a	ns

518

519 **Figure legends**

520 **Figure 1:** Ombrothermic diagram for natural and amplified drought in 2012, 2013 and 2014. Bars represent
521 mean monthly precipitation (mm) and curves represent mean monthly temperature (°C). On each amplified
522 drought graph, the percentage represents the proportion of excluded rain compared to natural drought plot.

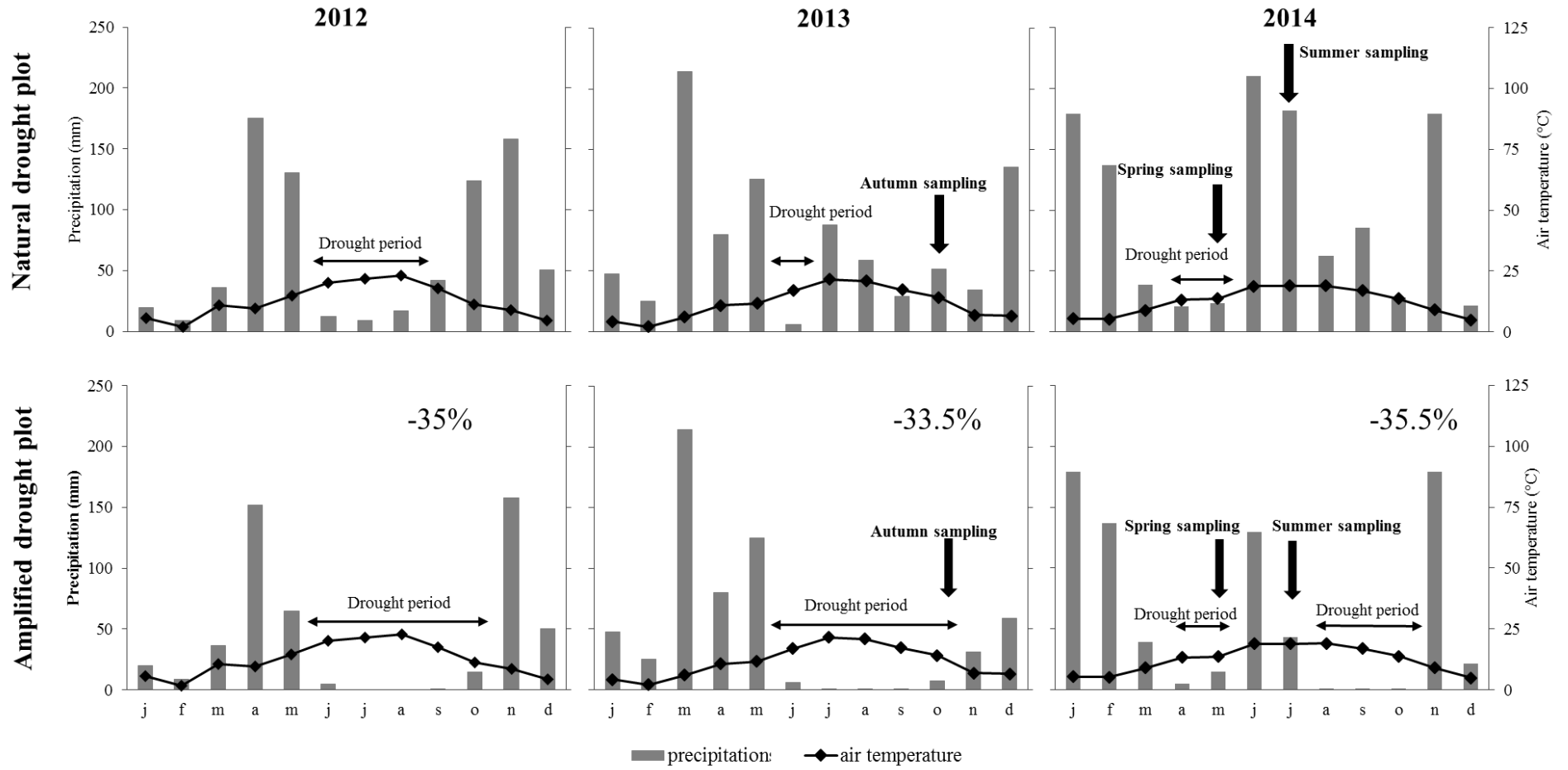
523
524 **Figure 2:** Diurnal pattern of stomatal conductance (G_w) and net photosynthesis (P_n) according to drought
525 treatment and season. Values showed represent means \pm SE, n=5.

526
527 **Figure 3:** Diurnal pattern of isoprene emissions rates, where points represent measured emissions, and the
528 yellow line correspond to modelled emissions rates according to the $L+T$ algorithm (ER_{L+T}). Values are mean \pm
529 SE, n=5. R^2 and slope (sl) of correlations between measured and modelled emissions are presented in the yellow
530 frame. Correlations were obtained without forcing data through the origin.

531
532 **Figure 4:** Diurnal pattern of acetaldehyde emissions rates, where points represent measured emissions, the
533 yellow line correspond to modelled emissions rates according to the $L+T$ algorithm (ER_{L+T}) and dotted line is
534 modelled emissions rates according to T algorithm (ER_T). Values are mean \pm SE, n=5. R^2 and slope (sl) of
535 correlations between measured and modelled emissions are presented in the yellow frame for $L+T$ and in the
536 white frame for T . Correlations were obtained without forcing data through the origin.

537
538 **Figure 5:** Diurnal pattern of measured methanol emissions rates. Points (means \pm SE, n=5) represent measured
539 emissions, yellow line correspond to modelled emissions rates according to the $L+T$ algorithm (ER_{L+T}) and
540 dotted line is modelled emissions rates according to T algorithm (ER_T). Values are mean \pm SE, n=5. R^2 and slope
541 (sl) of correlations between measured and modelled emissions are presented in the yellow frame for $L+T$ and in
542 the white frame for T . Correlations were obtained without forcing data through the origin.

543
544
545
546
547
548
549
550
551
552
553
554

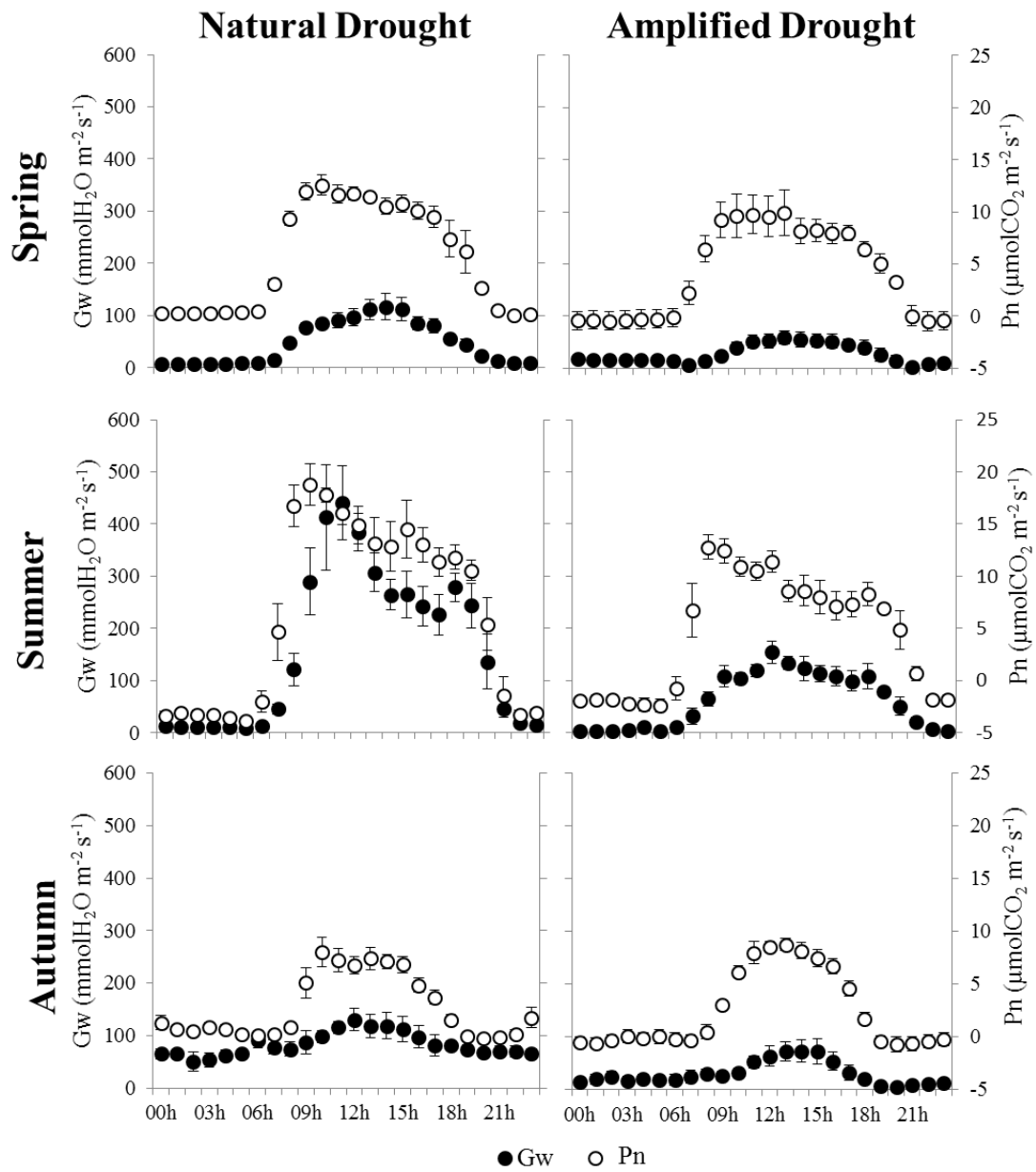


555

556 **Figure 1:**

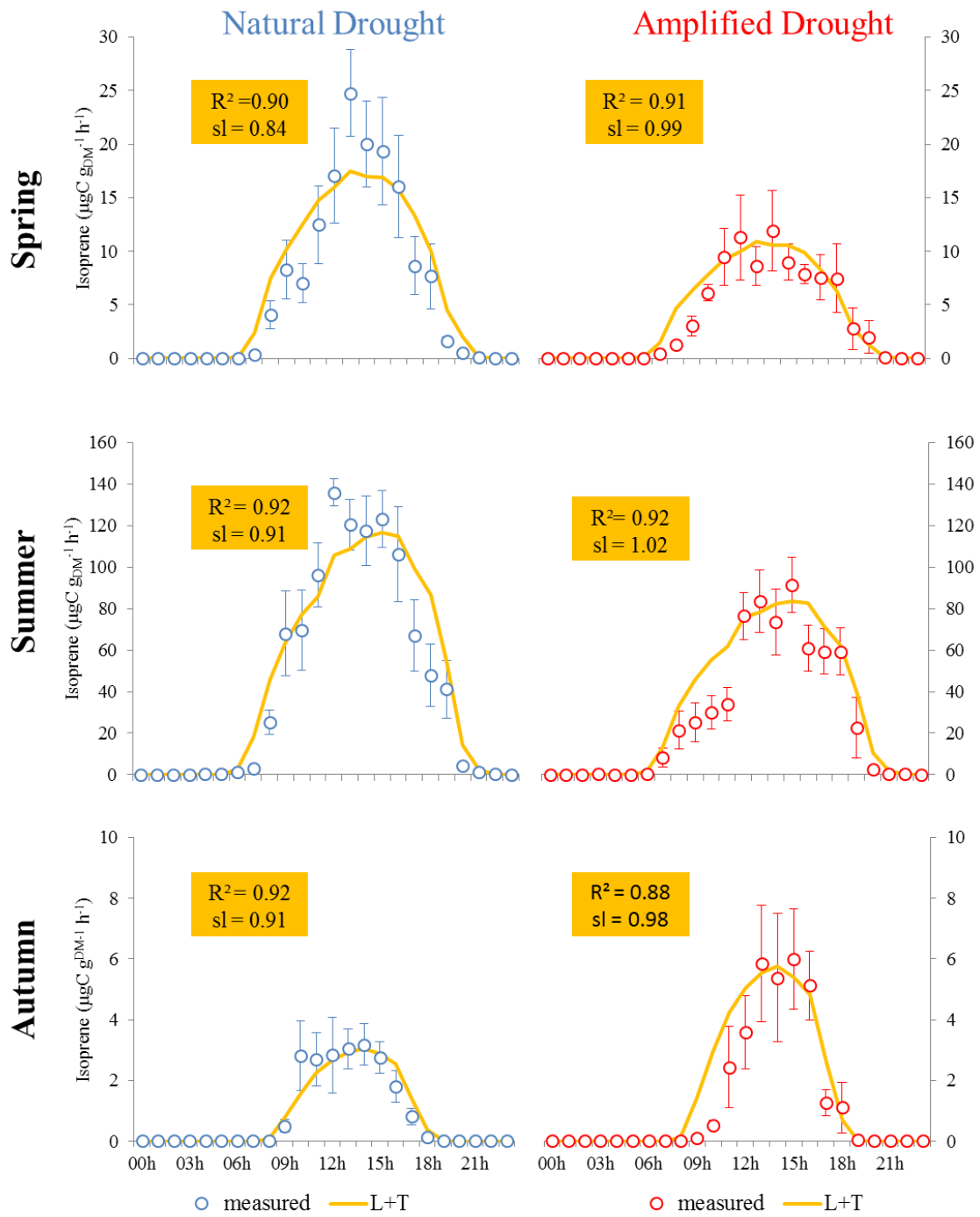
557

558



560

561 **Figure 2:**

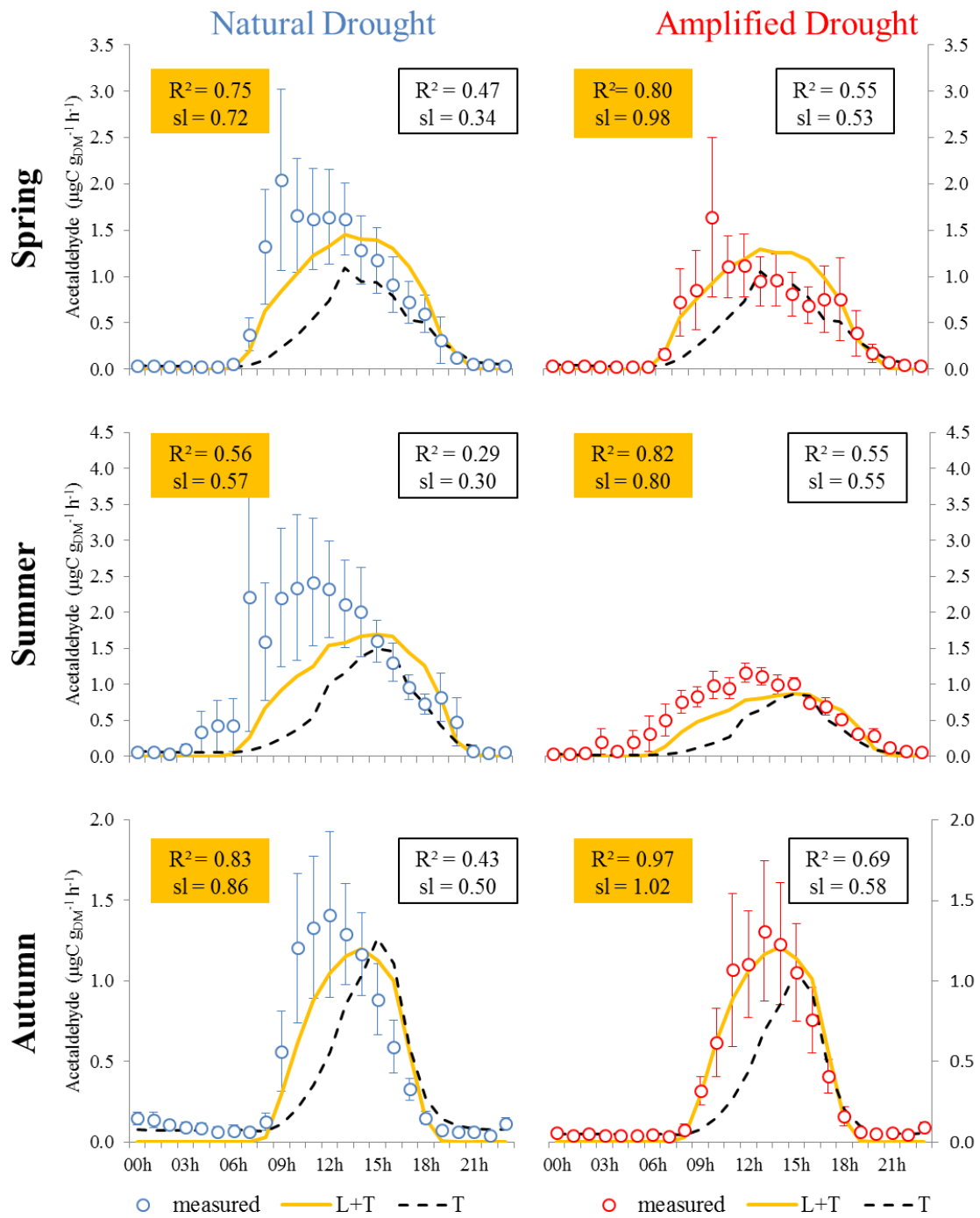


562

563 **Figure 3:**

564

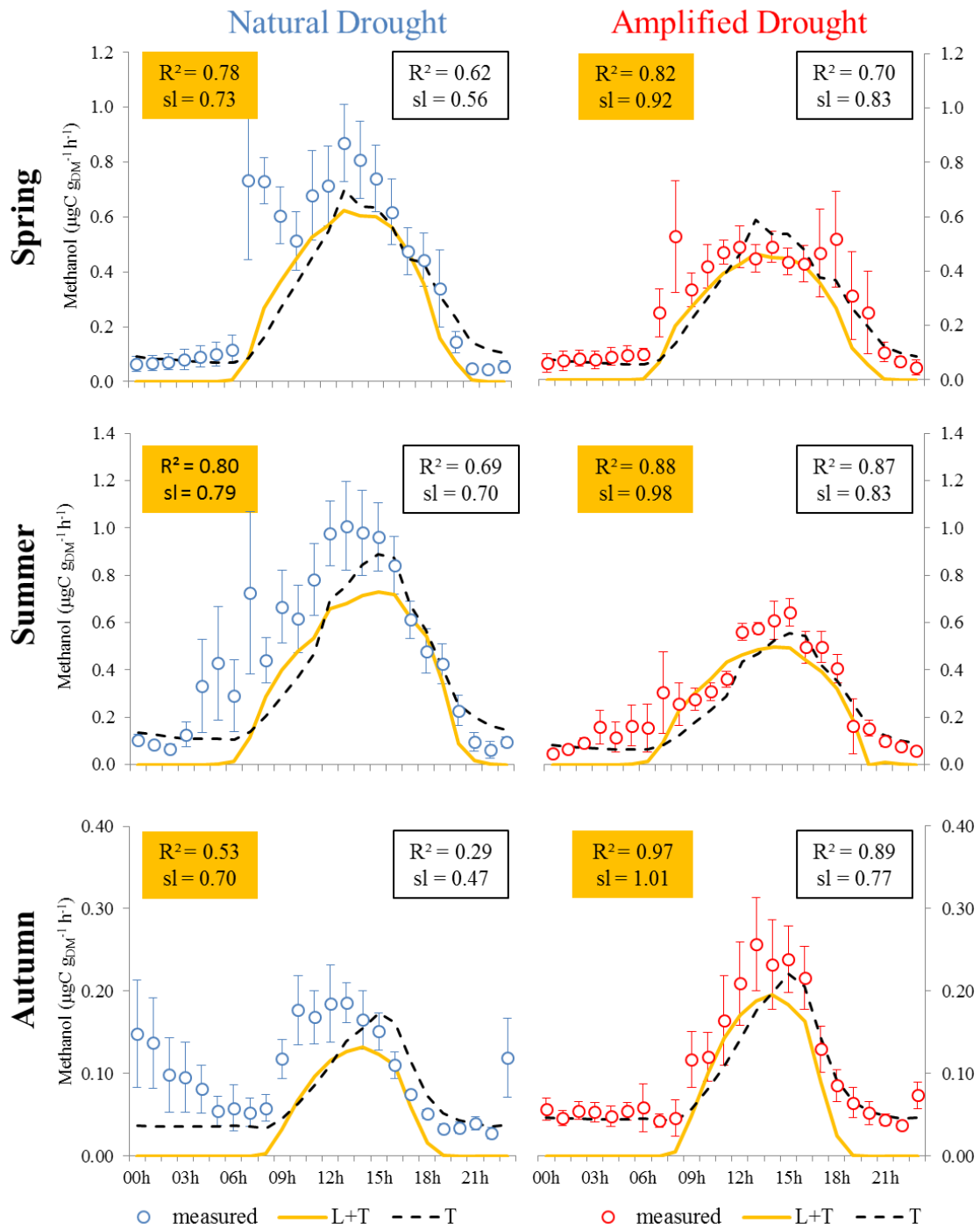
565



566

567 **Figure 4:**

568



569

570 **Figure 5:**

571

572

573

574

575